Coordinated regulation of synthesis and stability of RNA during the acute TNF-induced proinflammatory response

Michelle T. Paulsen[a], Artur Veloso[a,b], Jayendra Prasad[a], Karan Bedi[a,c], Emily A. Ljungman[a], Ya-Chun Tsan[a,c], Ching-Wei Chang[a,d], Brendan Tarrier[e], Joseph G. Washburn[e], Robert Lyons[e], Daniel R. Robinson[f], Chandan Kumar-Sinha[f], Thomas E. Wilson[f,g], and Mats Ljungman[a,c,1]

[a]Department of Radiation Oncology, University of Michigan Comprehensive Cancer Center and Translational Oncology Program, [b]Bioinformatics Program, Department of Computational Medicine and Bioinformatics, [c]Department of Environmental Health Sciences, School of Public Health, [d]Biomedical Engineering, [f]Department of Pathology, [g]Department of Human Genetics, and [e]University of Michigan DNA Sequencing Core, University of Michigan, Ann Arbor, MI 48109

Edited by Roy Parker, University of Colorado, Boulder, CO, and approved December 20, 2012 (received for review November 5, 2012)

Steady-state gene expression is a coordination of synthesis and decay of RNA through epigenetic regulation, transcription factors, micro RNAs (miRNAs), and RNA-binding proteins. Here, we present bromouride labeling and sequencing (Bru-Seq) and bromouridine pulse-chase and sequencing (BruChase-Seq) to assess genome-wide changes to RNA synthesis and stability in human fibroblasts at homeostasis and after exposure to the proinflammatory tumor necrosis factor (TNF). The inflammatory response in human cells involves rapid and dramatic changes in gene expression, and the Bru-Seq and BruChase-Seq techniques revealed a coordinated and complex regulation of gene expression both at the transcriptional and posttranscriptional levels. The combinatory analysis of both RNA synthesis and stability using Bru-Seq and BruChase-Seq allows for a much deeper understanding of mechanisms of gene regulation than afforded by the analysis of steady-state total RNA and should be useful in many biological settings.

The acute inflammatory response is critical for the defense against infections and in the healing of damaged tissues (1). The orchestration of the reprogramming of gene expression associated with the acute inflammatory response is complex and involves both transcriptional and posttranscriptional regulation (2–5). Conventional exploration of gene expression using total RNA does not fully capture this complexity because it does not provide insight into the contribution of nascent RNA synthesis or RNA decay to steady-state RNA changes. A number of different approaches have recently been developed to assess nascent RNA synthesis in cells such as global run-on and sequencing (GRO-Seq) (6), native elongating transcript sequencing (NET-Seq) (7), nascent RNA sequencing (Nascent-Seq) (8), and metabolic labeling of nascent RNA by using microarrays (9) or RNA-Seq (10, 11). By comparing the data obtained with metabolically labeled nascent RNA with the steady-state RNA levels, the rates of degradation of all transcripts can be computationally estimated. The stability of steady-state RNA can also be estimated from the decay rate of steady-state RNA after transcription inhibition (12–14) or by immunoprecipitation of metabolically labeled steady-state RNA after different chase periods (15, 16). These approaches work well when the system is at homeostasis, but not when conditions are altered by environmental stimuli or stress, such as the induction of the acute inflammatory response, when the rates of decay of transcripts are expected to change (10, 11).

In this study, we present Bru-Seq and BruChase-Seq based on bromouridine pulse labeling of nascent RNA followed by chases in uridine to obtain RNA populations of specific ages. The Bru-labeled RNA is then immunocaptured followed by deep sequencing. These techniques allowed us to assess changes in the rates of both synthesis and degradation of RNA globally after the activation of the proinflammatory response by TNF. Our results provide a comprehensive and complex picture of the contribution of transcriptional and posttranscriptional regulation during homeostasis and in the reprogramming of gene expression during the acute TNF-induced proinflammatory response.

Results

Metabolic Labeling of Nascent RNA with Bromouridine. To explore the contributions of both transcriptional and posttranscriptional regulation to the acute proinflammatory response, we developed Bru-Seq and BruChase-Seq. These approaches are based on a short labeling (30 min) of nascent RNA with bromouridine (Bru), followed by direct isolation (Bru-Seq) or a chase in uridine for different periods of time (BruChase-Seq). After labeling and chase, the Bru-containing RNA is specifically isolated from total RNA by using anti-BrdU antibodies. This material is then converted into a strand-specific cDNA library and subjected to deep sequencing followed by analysis of mapped read density across the reference genome (Fig. 1*A*). Bromouridine has been used to label nascent RNA (9, 17) or steady-state RNA (15) in cells or in vitro (6) followed by capturing of Bru-labeled RNA using specific anti-BrdU antibodies, and it is less toxic to cells than the analogs 4-thiouridine and ethynyluridine (15). The BruChase-Seq approach is unique in that the nascent RNA pool is labeled followed by uridine chases for different periods of time, making it possible to analyze RNA populations of distinct ages.

Incubation of human fibroblasts with 2 mM bromouridine for 30 min gave a robust RNA incorporation as measured by immunocytochemistry using anti-BrdU antibodies (*SI Appendix*, Fig. S1). As expected, this Bru incorporation was reduced by simultaneous incubation with the transcription inhibitors actinomycin D or 5,6-dichloro-1-β-D-ribofuranosylbenzimidazole (DRB). Moreover, removal of the bromouridine from the culture plates followed by a chase in 20 mM uridine resulted in the gradual disappearance of the nuclear signal as nascent RNAs are expected to be processed and exported out of the nucleus. The retention of some Bru signal even after a 2-h chase is most likely due to a continuation of bromouridine triphosphate (BrUTP) incorporation during the beginning of the chase until the supplied uridine is converted to UTP and to the extended time required to complete transcription of long genes.

The capturing of Bru-labeled RNA is performed by using anti-BrdU antibodies conjugated to magnetic beads. The amount of

Author contributions: M.T.P., J.P., T.E.W., and M.L. designed research; M.T.P., K.B., E.A.L., Y.-C.T., C.-W.C., and M.L. performed research; M.T.P., A.V., B.T., J.G.W., R.L., D.R.R., C.K.-S., T.E.W., and M.L. contributed new reagents/analytic tools; A.V., J.P., K.B., B.T., J.G.W., R.L., D.R.R., C.K.-S., T.E.W., and M.L. analyzed data; and T.E.W. and M.L. wrote the paper.

The authors declare no conflict of interest.

This article is a PNAS Direct Submission.

Data deposition: The sequence reported in this paper has been deposited in the Gene Expression Omnibus (GEO) database, www.ncbi.nlm.nih.gov/geo (accession no. GSE-43440).

[1]To whom correspondence should be addressed. E-mail: ljungman@umich.edu.

This article contains supporting information online at www.pnas.org/lookup/suppl/doi:10.1073/pnas.1219192110/-/DCSupplemental.

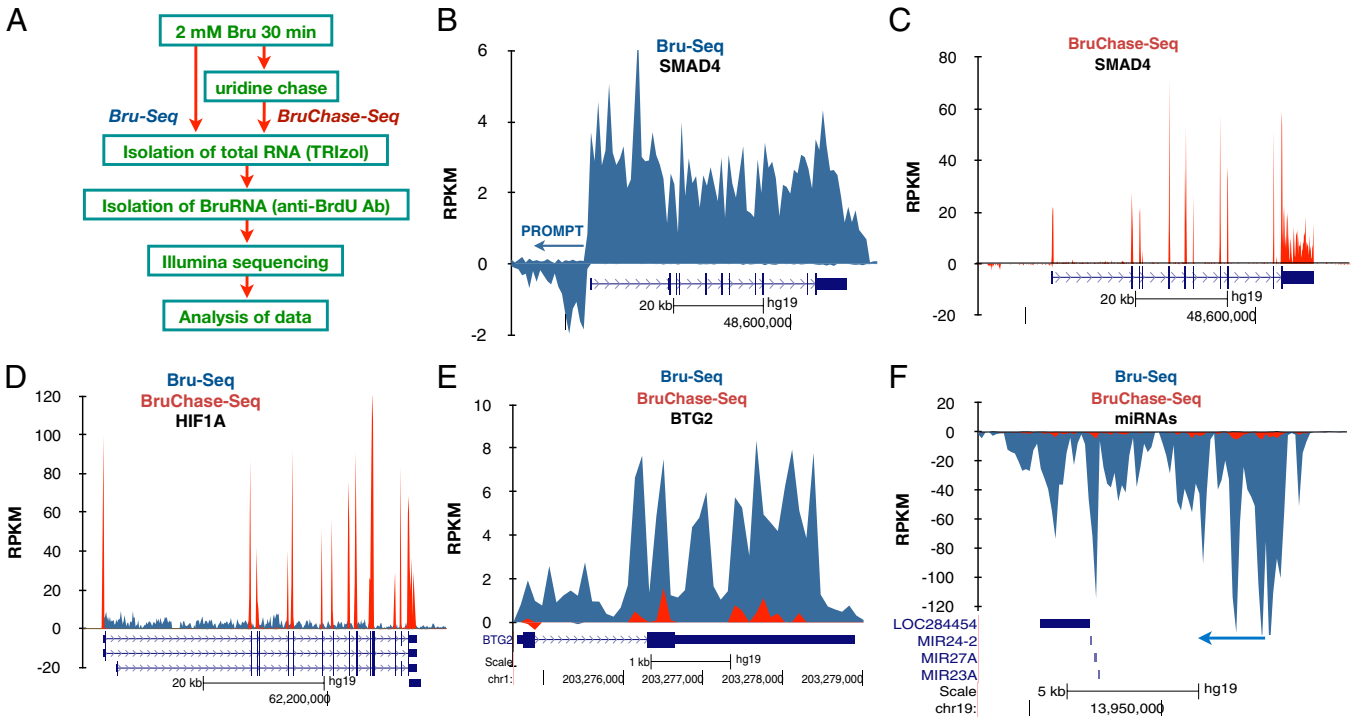

Fig. 1. Comparisons of nascent and 6-h-old RNA from human fibroblasts using Bru-Seq and BruChase-Seq. (*A*) Diagram illustrating the main steps in Bru-Seq and BruChase-Seq (see text for details). (*B*) Sequencing reads from nascent RNA (Bru-Seq) mapping to the *SMAD4* gene with reference sequence annotation below with exons and UTRs denoted as black lines. It can be noted that the nascent RNA maps to intronic and exonic sequences and to sequences beyond the 3′-end of the gene. Also, mapping of sequence reads on the opposite strand upstream of the *SMAD4* transcription start site represents divergent PROMPTs. (*C*) Sequence reads from 6-h-old *SMAD4* RNA (BruChase-Seq) (*D*) The ratio of the exonic signal in the 6-h old RNA to the signal throughout the gene in the nascent RNA reflects the relative stability of the mature RNA. The mature *HIF1A* transcript is an example of a stable transcript, whereas the *BTG2* transcript (*E*) is an example of an unstable transcript. (*F*) The primary transcripts of the *miR24-2*, *miR27A*, and *miR23A* microRNAs are clearly captured by using Bru-Seq but not when analyzing the 6-h-old RNA with BruChase-Seq implicating that the primary miRNA transcripts are rapidly processed into mature miRNAs and size excluded from our analysis. The gene maps are from RefSeq Genes [University of California, Santa Cruz (UCSC) genome browser, http://genome.ucsc.edu/].

unlabeled RNA captured as background with these antibody-conjugated beads was estimated to be below 0.4% (*SI Appendix*, Table S1). Notably, the isolated Bru-labeled RNA had a size distribution that differed markedly from the steady-state RNA from which it was captured (*SI Appendix*, Fig. S2). This size distribution is similar to what was reported for isolation of nuclear RNA in *Drosophila* cells (8).

Bru-Seq. Sequencing and mapping of cDNA libraries prepared from nascent RNA captured immediately after the 30-min Bru-labeling pulse (0-h) informs on where in the genome and at what rate transcription occurs across the cell population during the labeling period (the transcriptome). A description of all of the samples used and their mapping data can be found in *SI Appendix*, Table S2. As can be seen in Fig. 1*B* and *SI Appendix*, Fig. S3, the mapped reads from the nascent RNA covered entire genes, including both introns and exons. For some of the genes shown, reads could be detected on the opposite strand upstream of transcriptional start sites. This signal corresponds well to previously described promoter upstream transcripts (PROMPTs) (18), which are typically extremely short lived and not readily detectable by using steady-state RNA. This illustrates the power of Bru-Seq for detecting unstable transcripts.

The relative rate of transcription of genes within and between samples can be inferred by integrating the read signal throughout the gene and normalizing for the length of the gene and the total number of reads in the library to obtain "reads per thousand base pairs per 1 million reads" (RPKM). Because of ongoing splicing and degradation of intronic sequences during the labeling period, the integrated signal across the whole gene will be slightly underestimated. However, when the transcription rate of a particular gene is compared between two samples, this underestimation should not impact the estimation of the fold difference in expression between the two samples. The results obtained with Bru-Seq were highly reproducible when comparing different biological samples of the same cell line, and data from Bru-Seq correlated well with data obtained with the established in vitro run-on technique GRO-Seq on human lung fibroblasts (*SI Appendix*, Figs. S4 and S5). The transcriptome data for all genes (>300 bp) in human fibroblasts using Bru-Seq can be found in *SI Appendix*, Table S3. The highest transcribed gene in growing human fibroblasts was *MALAT1*, which encodes a nuclear noncoding RNA (ncRNA) thought to promote alternative splicing of various transcripts (19). More than 4,000 annotated genes (~20%) were silent at our level of detection in human fibroblasts.

BruChase-Seq. By chasing Bru-treated cells with uridine, RNA populations of defined ages can be obtained and many features of transcription, splicing, and RNA degradation can be observed with a clarity not afforded by other techniques. We obtained similar ranking order of the intrinsic stabilities of most transcripts by using a 2-h or a 6-h chase (*SI Appendix*, Fig. S6). However, because the length of a gene, i.e., the time it takes to complete transcription, and the lag time for effective uridine quenching of the BrUTP pool may influence the assessment of RNA stability when using short chase periods, we decided to use a 6-h chase for all subsequent BruChase-Seq experiments. We find close correlation between data obtained with BruChase-Seq and with quantitative RT-PCR (*SI Appendix*, Fig. S7). As can be seen in Fig. 1*C*, the 6-h-old Bru-labeled SMAD4 RNA was highly enriched for exons, consistent with maturation by splicing. By comparing the RPKM values of the exons in the 6-h-old sample with the RPKM values throughout the gene in the nascent

RNA sample, the intrinsic stability of a transcript can be estimated. An example of a stable transcript is *HIF1A* (Fig. 1*D*) and an example of an unstable transcript is *BTG2* (Fig. 1*E*). A list of relative intrinsic stabilities of transcripts in human fibroblasts can be found in *SI Appendix*, Table S3. Finally, highly unstable primary miRNA transcripts were readily detected when sequencing nascent RNA (Bru-Seq) but not when sequencing 6-h-old RNA (BruChase-Seq). An example is shown in Fig. 1*F* for the transcript of the *miR23-A*, *miR24-2*, and *miR27* cluster.

Genome-Wide Analyses. When analyzing the distribution of sequence reads throughout the genome of human fibroblasts, 10% of the Bru-Seq reads came from exonic regions, 75% from intronic regions, 3% was antisense RNA, and 12% came from unannotated, intergenic regions (Fig. 2*A*). The distribution of reads of the 6-h-old RNA with BruChase-Seq showed that the relative abundance of exonic reads increased to 49%, whereas intronic reads decreased to 24% reflecting the higher stability of exons relative to introns. Using a hidden Markov model (HMM) segmentation analysis to map all transcription units independently of prior gene annotations (*SI Appendix, SI Materials and Methods*), we were able to estimate that approximately 34% of the fibroblast genome was giving rise to a detectable transcription signal, whereas 66% of the genome did not generate any signal detectable above background (Fig. 2*B* and *SI Appendix*, Table S4). Thus, at our sequencing depth and growth conditions, we estimate that the "transcriptome" in human fibroblasts is confined to approximately 34% of the genome, which is in concordance with recent reports using a similar HMM segmentation approach for other human cell lines (20).

When plotting the transcriptome against the RNA stabilome of both mRNAs and annotated ncRNAs, we did not observe a clear relationship between relative transcription rate and relative RNA stability (Fig. 2*C*). The distribution of transcription rates and stabilities of mRNAs and annotated ncRNAs were fairly similar, suggesting that synthesis and turnover of mRNA and ncRNAs may be regulated by similar mechanisms as recently suggested (15, 21). Examples of the relative synthesis and stability of a set of ncRNAs can be found in *SI Appendix*, Fig. S8. By performing DAVID gene ontology analysis to test for gene enrichment, we found that genes involved in the KEGG pathway "ribosome" were significantly enriched in the highest transcribed gene set ($P < 6.84 \times 10^{-54}$) (Fig. 2*D* and *SI Appendix*, Figs. S9 and S10). Interestingly, the "ribosome" pathway was also highly enriched in the gene set of the least stable transcripts ($P < 1.37 \times 10^{-52}$). This finding that transcripts from ribosomal protein genes are very unstable concur with a study in *Saccharomyces cerevisiae* (22) and suggests a unique mechanism whereby cells regulate ribosome biogenesis. In addition, 14 of the 100 most highly transcribed genes were found to generate transcripts that were among the 100 least stable transcripts. These genes were *CYR61, DUSP1, DUSP6, EGR1, EID3, FAM43A, FOS, FOSB, ID1, JUN, JUNB, KLF6, MCL1,* and *ZFP36*.

Analysis of RNA Synthesis and Stability of Mitochondrial and Ribosomal RNA. The human mitochondrial genome is circular and consists of 16,569 bp encoding 8 mRNAs, 2 rRNAs, and 22 tRNAs (23). The

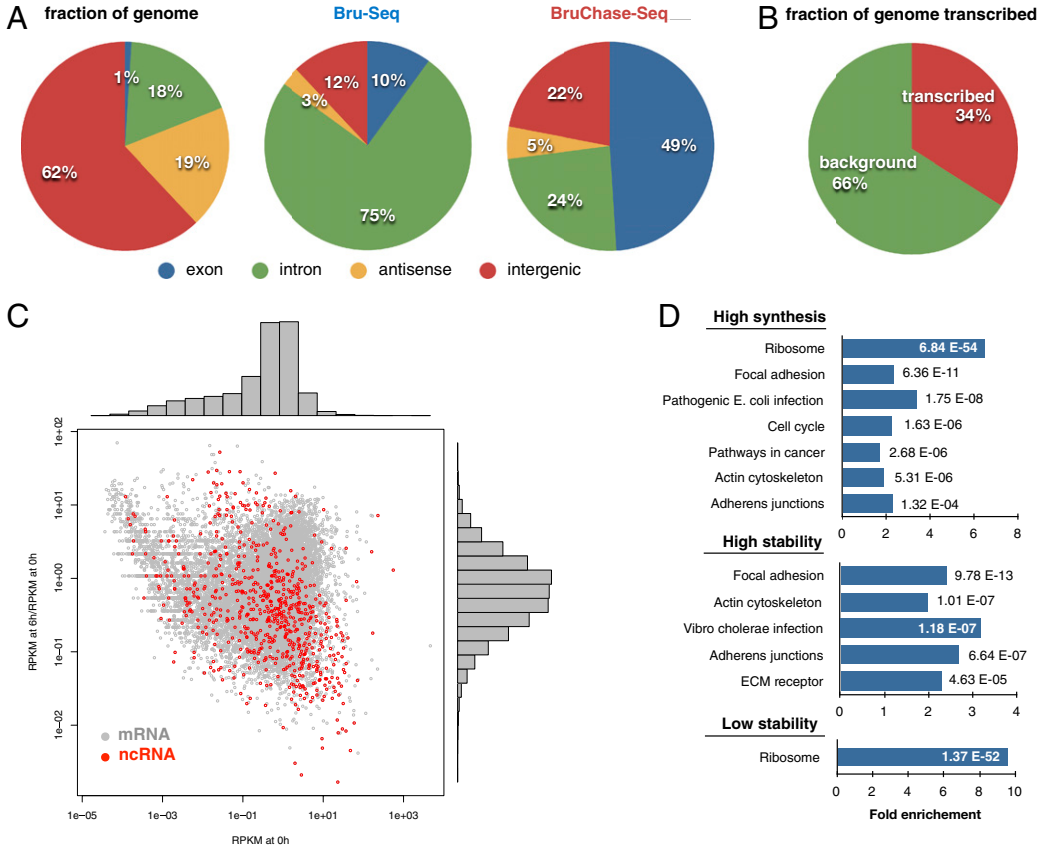

Fig. 2. Genomic distribution of sequencing reads obtained with Bru-Seq and BruChase-Seq. (*A Left*) The relative size of exonic, intronic, antisense, and intergenic compartments in the human genome. (*A Center*) Relative distribution of sequencing reads in these four compartments for nascent RNA (Bru-Seq). (*A Right*) Relative distribution of sequencing reads from the four different compartments for 6-h-old RNA (BruChase-Seq). (*B*) Assessment of the portion of the genome generating transcripts using a HMM segmentation analysis. (*C*) The transcriptome vs. the RNA stabilome with the RPKM values for synthesis (0-h) plotted against the relative stability score (6-h/0-h) for mRNAs (gray circles) and ncRNAs (red circles). (*D*) KEGG pathway gene enrichment analysis using the DAVID bioinformatics resource showing fold enrichment and *P* values for pathways enriched in the top 2,000 highly transcribed genes (*Top*), the top 2,000 most stable transcripts (*Middle*), and the 2,000 least stable transcripts (*Bottom*).

observation that the steady-state levels of the individual transcripts differ greatly despite being transcribed in a polycistronic fashion indicates that the levels of these transcripts must be under post-transcriptional regulation (24). Using BruChase-Seq, we directly assessed the relative stability of the mitochondrial RNAs. Although the two mitochondrial-encoded ribosomal RNAs, *RNR1* and *RNR2*, showed high relative stability, the transcripts of the protein-coding genes were highly unstable (*SI Appendix*, Fig. S11*A*, red trace).

To assess the synthesis and stability of rRNA in human fibroblasts, we first collapsed the ~400 rDNA genomic repeat sequences into one rDNA sequence and aligned all of the reads to this single locus as described (25). Significant processing of intergenic spacer RNA in the primary rRNA transcript is apparent (*SI Appendix*, Fig. S11*B*, blue trace). Because of a size selection step of cDNA before sequencing, we did not obtain sufficient amounts of the short 5.8S RNA for our analysis. The rRNA transcripts 18S and 28S showed an expected high stability relative to all other transcripts (*SI Appendix*, Fig. S11*B*, red trace). When calculating the contribution of mRNA and rRNA to the total pool of nascent RNA reads, rRNA made up approximately 10% and mitochondrial RNA approximately 7% (*SI Appendix*, Fig. S11*C*). These numbers increased to 38% and 9%, respectively, when analyzing the pool of 6-h-old RNA reflecting their overall relative stability.

Intron Retention. We observed a number of genes that produced transcripts where specific introns were retained even after a 6-h chase. (*SI Appendix*, Fig. S12 *A–D*). A strong correlation was found between the intron retention fraction, defined as the signal in an intron relative to the exons of the same gene, and the fraction of reads crossing the boundaries of the intron that were unspliced, indicating that these intronic reads originated from introns retained in the transcripts rather than from reduced rates of degradation of spliced introns. We found 360 introns that were retained to more than 10% in the 6-h-old RNA (*SI Appendix*, Fig. S12*E* and Table S5). Of these introns, 116 were found on genes with at least one additional retained intron, suggesting that when one intron is poorly spliced, there is a high likelihood that an additional intron will be poorly spliced. According to DAVID gene ontology analysis, the gene list of transcripts with retained introns was highly enriched in "phosphoproteins" ($P < 1.7 \times 10^{-20}$).

TNF-Induced Transcriptome. We next applied Bru-Seq to explore alterations in the transcriptome after an acute exposure to the inflammatory cytokine TNF in human fibroblasts. It is well known that the proinflammatory response involves dramatic changes in RNA levels in cells, and these changes are thought to be due to both transcriptional and posttranscriptional regulation (2–5). We first performed time course experiments with Bru labeling of nascent RNA and observed dramatic induction of nascent RNA synthesis already after 30 min of TNF treatment. The induction of nascent RNA synthesis for these genes peaked at 2–6 h after addition of TNF (Fig. 3*A* and *B*). Performing a genome-wide Bru-Seq data analysis of TNF-induced and repressed genes by using DESeq analysis (26), we found that 472 genes were up-regulated and 204 genes down-regulated at least twofold after a 1-h incubation with TNF (*SI Appendix*, Table S6). Examples of up-regulated genes were *IL1A* and *IL1B*, whereas *HES1* and *KLF4* represent genes down-regulated at the level of RNA synthesis (Fig. 3 *C–F*).

TNF-Induced RNA Stabilome. The rapid changes in gene expression after the induction of the proinflammatory response in human fibroblasts treated with TNF have been shown to depend on the induction of synthesis of genes with low intrinsic transcript stability (5). We first assessed the intrinsic stability of inflammation-associated transcripts by using the bromouridine pulse–chase strategy coupled to real-time RT-PCR arrays, and we confirmed that many of the proinflammatory genes generated very unstable transcripts (Fig. 3*G*) (5). We next assessed whether exposure to TNF may affect the stability of these transcripts in unperturbed cells by using the bromouridine pulse–chase approach. Cells were pulse labeled for 30 min in the absence of TNF and were then chased for 6 h in the presence or absence of TNF and, as can be seen, TNF dramatically increased the stability of many of these transcripts (Fig. 3*H*). We next used BruChase-Seq to examine the effect of TNF on RNA stability genome-wide and detected significantly increased stabilities of 152 transcripts, such as *SOD2* and *ICAM1* (Fig. 3 *I* and *J* and *SI Appendix*, Table S6). We also observed 58 transcripts significantly destabilized by TNF treatment after Bru labeling, such as *GAS1* and *HOXA9* (Fig. 3 *K* and *L*). Other members of the HOXA gene cluster, such as *HOXA6*, *HOXA11*, *HOXA13*, and *HOTAIR*, also showed reduced transcript stability after TNF treatment during the chase.

Coordinated and Complex Regulation of the Transcriptome and RNA Stabilome After TNF. The results show that cells induce the acute proinflammatory response by regulating both synthesis and stability of RNA. Some genes were found to be up-regulated transcriptionally, posttranscriptionally, or both. Other genes were down-regulated transcriptionally, posttranscriptionally, or both, or through a mixture of up- and down-regulation (*SI Appendix*, Figs. S17–S22). We also observed dramatic induction of primary transcripts of *miR155*, *miR146A*, and *miR3142* and repression of *miR143*, *miR145*, and *miR614* (*SI Appendix*, Fig. 23 *A* and *B*) after a 1-h TNF treatment. *miR155* and *miR146* have been shown to be induced by NFkB during inflammation (27, 28), and *miR155* has been shown to suppress *miR143* (29).

Finally, in very large genes with affected transcription after TNF treatment, we could "visualize" the wave of induced or repressed transcription moving through the gene. For the 300-kb-long *FNDC3B*, we observed that the front of the induced transcription wave had reached approximately 260 kb into the gene during the 90-min experiment (*SI Appendix*, Fig. S24). For the *TOX* gene, we saw reduced RNA synthesis in the first 180 kb into the gene, suggesting reduced initiation and then the spread of reduced transcription into the gene. The transcription signal from the *SAMD4A* gene showed a "hump," suggesting that this gene was transiently induced after TNF exposure.

By performing DAVID gene ontology enrichment analysis on the genes that were induced at the transcriptional and/or post-transcriptional level by TNF treatment, we found a number of pathways affected by TNF (Fig. 4). Bru-Seq showed more than 470 genes induced by TNF, and they were enriched in pathways that are known to be induced as part of the acute proinflammatory response such as "inflammation," "cytokine production," and "antiapoptosis". In addition, Bru-Seq detected more than 200 genes being repressed rapidly after TNF exposure and these genes were enriched in pathways such as "negative regulation of transcription," "nucleosome core," and "ubiquitin conjugation." Using BruChase-Seq, we found that more than 200 genes were regulated posttranscriptionally after TNF treatment, and some of these pathways were in common with those affected transcriptionally such as "inflammatory response," "response to wounding," and "antiapoptosis."

Discussion

TNF is an important proinflammatory cytokine that mediates its biological effects by activating NFkB, AP-1, and p38 (30, 31). NFkB and AP-1 are transcription factors regulating transcription initiation, whereas p38 is a kinase that has been shown to regulate mRNA stability by phosphorylating RNA-binding proteins such as tristetraproline (3). Numerous studies have profiled TNF-induced gene expression and mRNA stabilization in different cells by using steady-state RNA and the transcription inhibitor actinomycin D. However, actinomycin D induces cellular stress responses involving p53 (32) and have been shown to introduce artifacts in mRNA stability determinations (16, 33). In this study, we developed Bru-Seq and BruChase-Seq to profile the transcriptome and RNA stabilome of unperturbed human

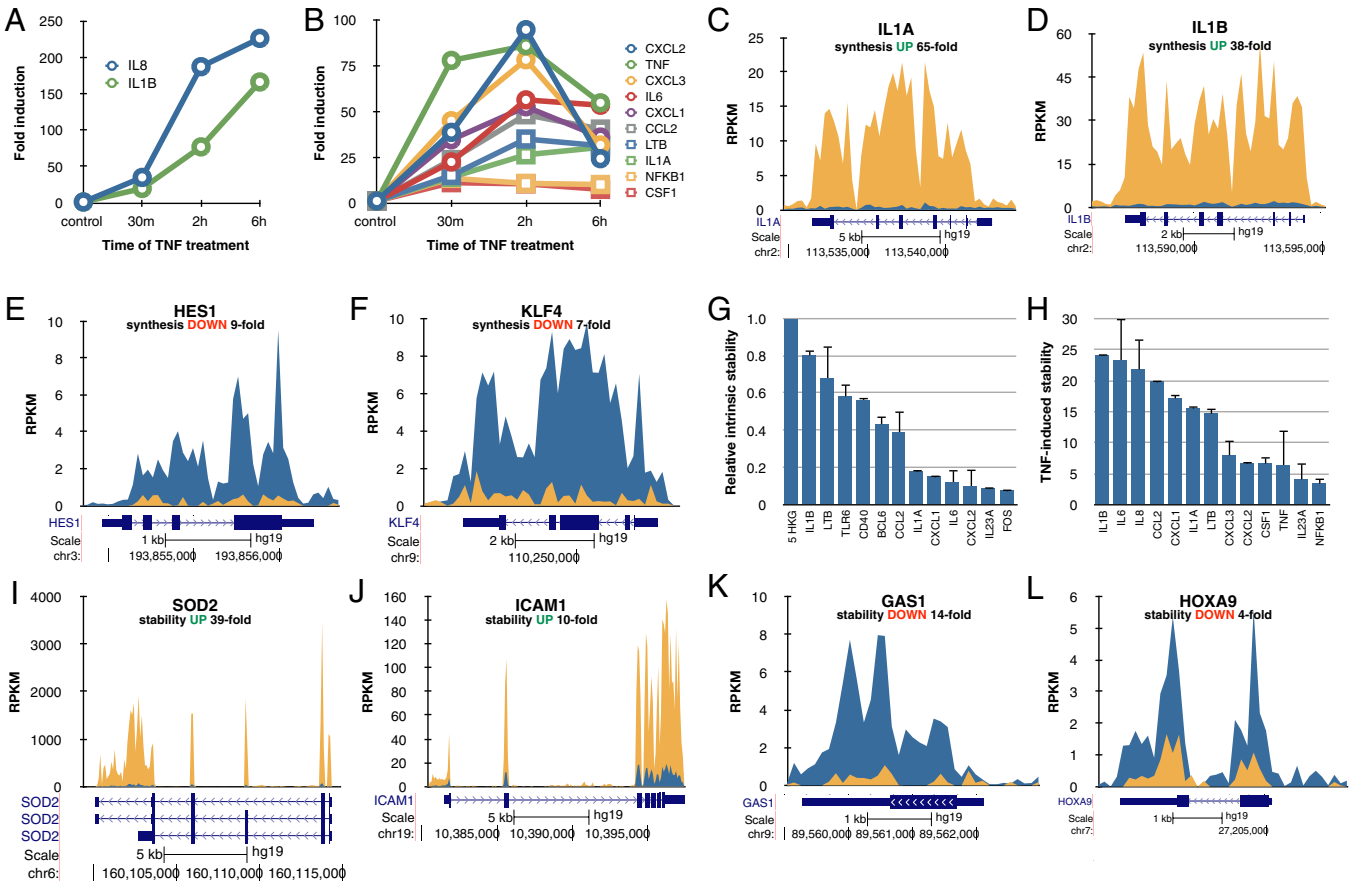

Fig. 3. Effects of TNF on the synthesis and stability of RNA. (*A* and *B*) Human fibroblasts were treated with 10 ng/mL TNF for different periods of time at 37 °C with 2 mM bromouridine present during the last 30 min. Total RNA was isolated and Bru-containing RNA isolated by using anti-BrdU antibodies and analyzed by using real-time RT-PCR array technology (inflammation and autoimmunity RT-PCR array; SABiosciences). The values represent the average of two independent experiments. (*C* and *D*) TNF-induced transcription of IL1A and IL1B. Blue color represent control, and yellow represent a 60+30 min treatment with TNF. (*E* and *F*) Rapid down-regulated transcription of the *HES1* and *KLF4* genes by TNF. (*G*) Intrinsic RNA stability of inflammatory cytokine RNAs. Human fibroblast were incubated with 2 mM bromouridine for 30 min followed by a 6-h uridine chase, isolation of Bru-containing RNA from total RNA and real-time PCR analysis using RT-PCR array technology (inflammation and autoimmunity RT-PCR array; SABiosciences). The values are normalized to five housekeeping genes (5 HKG) on the array, which are set to 1.00, and they represents the average of two independent experiments with error bars showing the SD. (*H*) Same as in *G* but 10 ng/mL TNF was added at the beginning of the 6-h chase period. The relative abundance of a particular RNA after the 6-h chase in the presence of TNF was compared with its relative abundance after a 6-h chase in the absence of TNF. (*I* and *J*) TNF increased stability of the *SOD2* and *ICAM* transcripts. Blue color represents control 6-h chase and yellow represent TNF treatment during the 6-h chase (*K* and *L*) TNF treatment resulted in the de-stabilization of the *GAS1* and *HOXA9* transcripts. The gene maps are from RefSeq Genes (UCSC genome browser, http://genome.ucsc.edu/).

skin fibroblasts at homeostasis and after induction of the proinflammatory response by TNF treatment.

Our results revealed that the TNF-induced proinflammatory response elicits a coordinated and complex reprogramming of gene expression by induction or repression of transcription and/or RNA stability. It was noticeable that many of the proinflammatory cytokines and chemokines were induced both transcriptionally and posttranscriptionally by TNF. It is possible that this dual induction occurs as a result of the activation of two separate signaling arms, such as NFkB for induction of gene-specific transcription and p38 kinase for promoting RNA stabilization via phosphorylation of specific RNA-binding proteins. Alternatively, the reduced decay of these transcripts may be due to "mass action" where the machinery that normally targets these transcripts for degradation becomes overwhelmed by the dramatically increased amounts of transcripts generated.

The data obtained with the Bru-Seq and BruChase-Seq techniques provides a record of both ongoing transcription (transcriptome) and the rate of decay of the generated RNA (RNA stabilome). In addition, the approaches can determine splicing efficiencies genome-wide and detect and map the generation of short-lived RNA species such as PROMPTs and primary miRNA transcripts. Because the Bru-Seq approach only measures newly made RNA, rapid reduction in transcription rates can be estimated without relying on the decay of preexisting RNAs. Thus, our list of genes rapidly inhibited after TNF treatment is unique and should contribute to the understanding of the acute proinflammatory response. We believe that the Bru-Seq and BruChase-Seq techniques should have a wide utility in many biological settings were transcriptional and posttranscriptional regulation is desired to be assessed on a genome-wide scale.

Materials and Methods

Bromouridine Pulse–Chase Labeling and Isolation of Bru-RNA. Bromouridine (Aldrich) was added to the media of normal diploid fibroblasts to a final concentration of 2 mM, and cells were incubated at 37 °C for 30 min. Cells were then washed three times in PBS and either collected directly (nascent RNA, Bru-Seq) or chased in conditioned media containing 20 mM uridine for 6 h at 37 °C (6-h-old RNA, BruChase-Seq). For TNF treatments, recombinant human TNF-α (R&D Systems) was added to a concentration of 10 ng/mL from a 10 μg/mL stock solution in PBS either 1 h before (and included during) Bru-labeling (Bru-Seq) or directly after Bru-labeling during the 6-h uridine chase (BruChase-Seq). Total RNA was isolated by using TRIzol reagent (Invitrogen), and Bru-labeled RNA was isolated from the total RNA by incubation with anti-BrdU antibodies (BD Biosciences) conjugated to magnetic beads

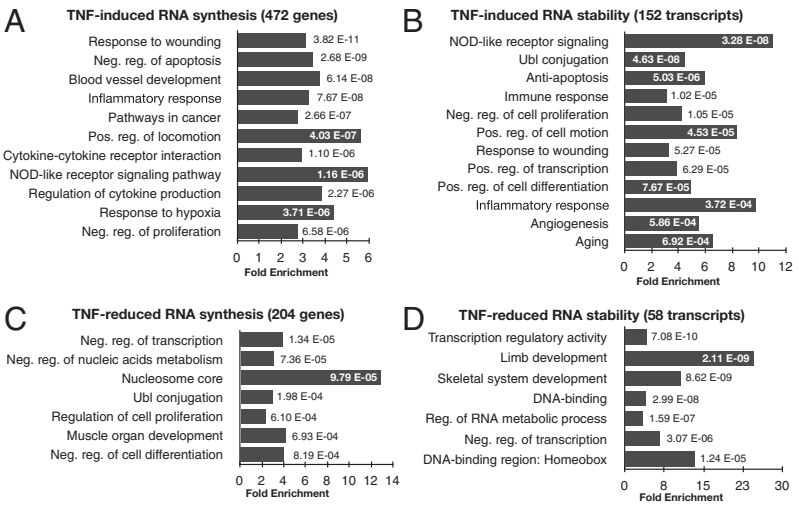

Fig. 4. Pathway enrichment analysis using DAVID gene ontology for genes affected transcriptionally or posttranscriptionally at least twofold by TNF treatment. (*A*) Pathway enrichment of genes induced transcriptionally (472 genes) or (*B*) posttranscriptionally (152 transcripts). (*C*) Pathway enrichment for genes repressed transcriptionally (204 genes) or (*D*) posttranscriptionally (58 transcripts). The bars represent fold enrichment of the particular pathway and are shown in order of significance (*P* values) listed on the right of the bars.

(Dynabeads, Goat anti-Mouse IgG; Invitrogen) under gentle agitation at room temperature for 1 h. For more detail, see *SI Appendix, SI Materials and Methods*.

cDNA Library Preparation and Illumina Sequencing. Isolated Bru-labeled RNA was used to prepare strand-specific DNA libraries by using the Illumina TruSeq Kit (Illumina) according to the manufacturer's instructions with modifications noted in *SI Appendix, SI Materials and Methods*. Sequencing of the cDNA libraries prepared from nascent RNA or 6-h-old RNA was performed at the University of Michigan Sequencing Core by using the Illumina HiSEq. 2000 sequencer.

Data Analysis and Availability. For details, see *SI Appendix, SI Materials and Methods*.

ACKNOWLEDGMENTS. We thank Manhong Dai and Fan Meng for administration and maintenance of the University of Michigan Molecular and Behavioral Neuroscience Institute computing cluster and the personnel at the University of Michigan Sequencing Core for technical assistance. This work was supported by funds from the University of Michigan Bioinformatics Program, the University of Michigan Biomedical Research Council, the Will and Jeanne Caldwell Endowed Research Fund of the University of Michigan Comprehensive Cancer Center, the University of Michigan School of Public Health via National Institute of Environmental Health Sciences Grant P30, the Department of Defense, Uniting Against Lung Cancer, the University of Michigan Nathan Shock Center, the University of Michigan Office of the Vice President of Research, and National Cancer Institute Grant 5R21CA150100, National Institute of Environmental Sciences Grant 1R21ES020946, and National Human Genome Research Institute Grant 1R01HG006786.

1. Medzhitov R (2008) Origin and physiological roles of inflammation. *Nature* 454(7203): 428–435.
2. Tian B, Nowak DE, Brasier AR (2005) A TNF-induced gene expression program under oscillatory NF-kappaB control. *BMC Genomics* 6:137.
3. Anderson P (2010) Post-transcriptional regulons coordinate the initiation and resolution of inflammation. *Nat Rev Immunol* 10(1):24–35.
4. Khabar KS (2010) Post-transcriptional control during chronic inflammation and cancer: A focus on AU-rich elements. *Cell Mol Life Sci* 67(17):2937–2955.
5. Hao S, Baltimore D (2009) The stability of mRNA influences the temporal order of the induction of genes encoding inflammatory molecules. *Nat Immunol* 10(3):281–288.
6. Core LJ, Waterfall JJ, Lis JT (2008) Nascent RNA sequencing reveals widespread pausing and divergent initiation at human promoters. *Science* 322(5909):1845–1848.
7. Churchman LS, Weissman JS (2011) Nascent transcript sequencing visualizes transcription at nucleotide resolution. *Nature* 469(7330):368–373.
8. Khodor YL, et al. (2011) Nascent-seq indicates widespread cotranscriptional pre-mRNA splicing in Drosophila. *Genes Dev* 25(23):2502–2512.
9. Ohtsu M, et al. (2008) Novel DNA microarray system for analysis of nascent mRNAs. *DNA Res* 15(4):241–251.
10. Rabani M, et al. (2011) Metabolic labeling of RNA uncovers principles of RNA production and degradation dynamics in mammalian cells. *Nat Biotechnol* 29(5):436–442.
11. Schwanhäusser B, et al. (2011) Global quantification of mammalian gene expression control. *Nature* 473(7347):337–342.
12. Lam LT, et al. (2001) Genomic-scale measurement of mRNA turnover and the mechanisms of action of the anti-cancer drug flavopiridol. *Genome Biol* 2(10):RESEARCH0041.
13. Raghavan A, et al. (2002) Genome-wide analysis of mRNA decay in resting and activated primary human T lymphocytes. *Nucleic Acids Res* 30(24):5529–5538.
14. Gerstein MB, et al. (2012) Architecture of the human regulatory network derived from ENCODE data. *Nature* 489(7414):91–100.
15. Tani H, et al. (2012) Genome-wide determination of RNA stability reveals hundreds of short-lived noncoding transcripts in mammals. *Genome Res* 22(5):947–956.
16. Munchel SE, Shultzaberger RK, Takizawa N, Weis K (2011) Dynamic profiling of mRNA turnover reveals gene-specific and system-wide regulation of mRNA decay. *Mol Biol Cell* 22(15):2787–2795.
17. Haider SR, Juan G, Traganos F, Darzynkiewicz Z (1997) Immunoseparation and immunodetection of nucleic acids labeled with halogenated nucleotides. *Exp Cell Res* 234(2):498–506.
18. Preker P, et al. (2008) RNA exosome depletion reveals transcription upstream of active human promoters. *Science* 322(5909):1851–1854.
19. Tripathi V, et al. (2010) The nuclear-retained noncoding RNA MALAT1 regulates alternative splicing by modulating SR splicing factor phosphorylation. *Mol Cell* 39(6): 925–938.
20. Djebali S, et al. (2012) Landscape of transcription in human cells. *Nature* 489(7414): 101–108.
21. Clark MB, et al. (2012) Genome-wide analysis of long noncoding RNA stability. *Genome Res* 22(5):885–898.
22. Grigull J, Mnaimneh S, Pootoolal J, Robinson MD, Hughes TR (2004) Genome-wide analysis of mRNA stability using transcription inhibitors and microarrays reveals posttranscriptional control of ribosome biogenesis factors. *Mol Cell Biol* 24(12): 5534–5547.
23. Asin-Cayuela J, Gustafsson CM (2007) Mitochondrial transcription and its regulation in mammalian cells. *Trends Biochem Sci* 32(3):111–117.
24. Mercer TR, et al. (2011) The human mitochondrial transcriptome. *Cell* 146(4):645–658.
25. Zentner GE, Saiakhova A, Manaenkov P, Adams MD, Scacheri PC (2011) Integrative genomic analysis of human ribosomal DNA. *Nucleic Acids Res* 39(12):4949–4960.
26. Anders S, Huber W (2010) Differential expression analysis for sequence count data. *Genome Biol* 11(10):R106.
27. O'Connell RM, Taganov KD, Boldin MP, Cheng G, Baltimore D (2007) MicroRNA-155 is induced during the macrophage inflammatory response. *Proc Natl Acad Sci USA* 104(5): 1604–1609.
28. Taganov KD, Boldin MP, Chang KJ, Baltimore D (2006) NF-kappaB-dependent induction of microRNA miR-146, an inhibitor targeted to signaling proteins of innate immune responses. *Proc Natl Acad Sci USA* 103(33):12481–12486.
29. Jiang S, et al. (2012) A novel miR-155/miR-143 cascade controls glycolysis by regulating hexokinase 2 in breast cancer cells. *EMBO J* 31(8):1985–1998.
30. Aggarwal BB (2003) Signalling pathways of the TNF superfamily: A double-edged sword. *Nat Rev Immunol* 3(9):745–756.
31. Beg AA, Baltimore D (1996) An essential role for NF-kappaB in preventing TNF-alpha-induced cell death. *Science* 274(5288):782–784.
32. Ljungman M, Zhang FF, Chen F, Rainbow AJ, McKay BC (1999) Inhibition of RNA polymerase II as a trigger for the p53 response. *Oncogene* 18(3):583–592.
33. Dölken L, et al. (2008) High-resolution gene expression profiling for simultaneous kinetic parameter analysis of RNA synthesis and decay. *RNA* 14(9):1959–1972.
34. Mortazavi A, Williams BA, McCue K, Schaeffer L, Wold B (2008) Mapping and quantifying mammalian transcriptomes by RNA-Seq. *Nat Methods* 5(7):621–628.